Microstructure and Mechanical Properties of Methane Hydrate-Bearing Sand

Thi Xiu Le[1](✉), Anh Minh Tang[1], Patrick Aimedieu[1], Michel Bornert[1], and Andrew King[2]

[1] Laboratoire Navier, Ecole des Ponts ParisTech, CNRS UMR 8205, Univ. Gustave Eiffel, Marne-la-Vallée, France
thi-xiu.le@enpc.fr

[2] Psiché beamline, Synchrotron SOLEIL, Paris, France

Abstract. Methane hydrates (MHs), solid ice-like compounds of methane gas and water, form naturally at high pressure and low temperature in marine or permafrost settings. They represent a great alternative energy resource but also a source of geo-hazards and climate change. Knowledge of physical/mechanical properties of sediments containing MHs, depending considerably on methane hydrate morphologies and distribution at the pore scale, is of major importance to be able to minimize the environmental impacts of future exploitation of methane gas from methane hydrate-bearing sands (MHBS). Much of the reported experimental work consists in laboratory tests on synthetic samples due to the extreme difficulty to get intact cored natural methane hydrate-bearing sediment samples. Various methods have been proposed to form methane hydrates in sandy sediments to mimic natural MHBS, but with limited success. This paper discusses the morphologies and pore habits of MHs formed in synthetic MHBS, considered as model materials for real MHBS and their effects on the mechanical properties of MHBS, at various scales and via different methods mainly as synchrotron X-ray computed tomography, magnetic resonance imaging and triaxial tests. An alternative MH formation method is proposed to better mimic natural MHBS and the validity of existing idealized models used to describe MH pore habits is discussed.

Keywords: Methane hydrate · Microstructure · Mechanical behaviors

1 Introduction

Natural gas hydrates (mainly methane hydrates), most often located in marine and permafrost settings, represent a great potential energy resource (estimates range over several orders of magnitude: ~3100 Tm^3 to ~7,650,000 Tm^3) but also a source of greenhouse gas (methane is an active "green-house" gas that has a global warming potential twenty times greater than an equivalent weight of carbon dioxide when integrated over 100 years) and geo-hazards (slope instability and wide-scale gas venting due to the dissociation of MHs replacing rigid components with free gas and excess water, which may significantly reduce the geo-mechanical stability of affected sediments) [1]. Detailed knowledge about

D. V. K. Huynh et al. (Eds.): VSOE 2021, LNCE 208, pp. 501–508, 2022.
https://doi.org/10.1007/978-981-16-7735-9_56

how released methane gas from MHs reaches atmosphere needs to be clarified as that is a key issue in understanding the connections between MH as an energy resource and also a potential player in future climate scenarios [2].

The formation of MH in sandy sediments modifies the microstructure and as consequence the physical/mechanical properties of MHBS. The study of the microstructure of MHBS, MH morphologies and distribution at the pore scale (pore habits), is of major importance in order to minimize the environmental impacts of future exploitation of methane gas from MHBS [2].

The majority of the existing experimental works focus on synthetic samples in laboratory due to challenges to get undisturbed cored MHBS samples. Various methods have been proposed to form MH in sandy sediments in laboratory and conceptual models proposed by Dvorkin et al. [3] have usually been used to indirectly assess the MH pore habits in sandy sediments [4–8]. Laboratory and synchrotron X-ray computed tomography (XRCT & SXRCT) have been recently used to investigate the microstructure of gas hydrate-bearing sediments [9–12]. It should be noted that due to the poor contrast between water and methane hydrate in a XRCT image, other types of gas or saline water solutions have been usually used.

In this paper, results obtained from the project HYDRE [13] on MH formation and its effects on the microstructure and the mechanical properties of synthetic MHBS under both excess-gas and excess-water conditions are discussed. The MH formation following the excess-gas method is first analyzed. Afterward, MH morphology and pore habit changes after the water saturation with or without an additional temperature cycle and their corresponding effects on the microstructure and the mechanical properties of MHBS are debated.

2 MH Formation Under Excess-Gas Conditions

2.1 MH Formation Procedure

In the project HYDRE [13], MHBS was formed following the partial water saturation method by injecting methane gas at 7 MPa and maintaining temperature at 3–4°, see [8, 12–14] for more details.

The initial water saturation was 25–50%. The stabilization of the compressional wave velocity (V_P) at the end of the MH formation suggested that almost the entire quantity of available water has been transformed into methane hydrates [8]. The final MH saturation increased with an increase in initial water in this range. Furthermore, two experiments at 25% of initial water saturation, observed by magnetic resonance imaging (MRI) [14], showed that almost 100% of water became MH in the end. Ten percent of volume increase was supposed for the water-methane hydrate conversion. However, in the work of Zhang et al. [15], 5 to 15% of pore water was found to remain unconverted to MH at the end of the experiments with 25–50% of initial water saturation. Actually, in these works, the signal of methane gas was not considered and that would induce errors in water content estimation in the specimen. In addition, the experiment duration was only few hours for these works compared to several days for triaxial and MRI tests in the present work [8, 13, 14].

2.2 MH Morphologies and Pore Habits Under Excess-Gas Conditions

The results of eight samples shown in Le et al. [8] show that MH formation in gas-saturated media increased V_p, and this increase reached the stabilization state at the end of the MH formation (before shearing). It was supposed that almost the distribution of MHs was similar to that of water prior to their creation. Comparison between the experimental data and Dvorkin's model [3] shown in Le et al. [8] suggests that at a low initial water saturation (MH saturation), methane hydrates were mainly distributed at grain surfaces (cementing - mineral coating), while at a high initial water saturation, the role of MHs at grain contacts (cementing - grain contacts) dominated. These macroscopic results are in agreement with that of Waite et al. [4] by using similar approaches (velocity measurements and Dvorkin's model). Note that the cementing - grain contacts model was only considered at low gas hydrate saturation.

At the pore scale, Zhao et al. [16] observed MHs (formed following the excess-gas method) at gas-water interfaces, floated between sand grains without coating on grain surfaces. A thick water layer was found to envelop grain surfaces by using image segmentation. Besides, polyhedral crystals of Xe hydrates around grains and loosely connected aggregates of Xe hydrate crystals in the pore space (formed following the excess-gas method), were observed by SXRCT [10]. Furthermore, thin layers of water were observed to exist between sand grains and Xe hydrates. It should be noted that the Xe hydrate formation time was just some ten minutes, remaining water could still be transformed into MHs. Furthermore, the morphology of gas hydrates depends on the type of used gas.

Within spatial resolution of sub-micron voxel size of SXRCT images in the work of Le et al. [12], MH morphologies and pore habits were observed directly without the need of segmentation (see Fig. 1a–d). That allows to discuss the four types of MH pore habits, proposed by Dvorkin et al. [3]: cementings, load-bearing and pore-filling, usually used for predictions of physical/mechanical behaviors of MHBS. It is usually supposed that MH formed under excess-gas conditions in sandy sediments (following the excess-gas or ice-seeding method) have the shape of pendular water menisci at grain-grain contacts or thin uniform MH layers coating sand surfaces (cementing - mineral coating) [4, 5]. The present study and that of Lei et al. [11] showed irregular shapes of MH at sand surfaces often accompanied by finger-like spreading patterns of MHs at low MH saturation. It appears that methane hydrates were at grain-grain contacts and/or grains surfaces (cementing) at low hydrate saturation while they tended to fill the pore space at high hydrate saturation. Besides, methane hydrates could be porous if they were not totally clogged over time. It is clear that MH morphologies and pore habits in the sample are not only heterogeneous at the pore scale but also along the sample height (the sample scale) due to water migrations [12]. Different types of MH morphologies and pore habits could exist in the sample. Not only MH pore habits but also MH morphologies in sandy sediments (which can only be observed at high image spatial resolution) are important for studies on physical/mechanical behaviors of methane hydrate-bearing sediments. At similar MH saturation, different MH morphologies (filaments, "crystals" or layers) at sand grain surfaces (cementing - mineral coating) or at contacts of grains (cementing - grain contacts) can play different roles in mechanical behaviors of methane hydrate-bearing sediments. We suppose here an intermediary model of MHs at the grain scale

(see Fig. 1e) with complex geometry of MHs that could eventually be porous. MHs could play more role at grain contacts compared to the conceptual cementing-mineral coating model by forming bulk MHs. Furthermore, effects of thin water film supposed existing between sand grain and MH on physical/mechanical behaviors of sediments have not been well studied yet. It seems vital that numerical studies on mechanical behaviors of MHBS, which have been based on four idealized MH pore habits, should take into account more realistic and less caricatural MH morphologies and pore habits.

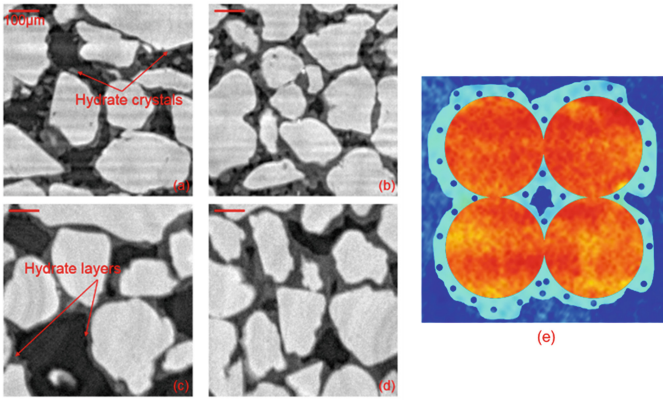

Fig. 1. Some examples of real MH microstructure in MHBS under excess-gas conditions (a–d); (e): An alternative model of MH pore habits under excess-gas conditions (Blue: methane gas; Cyan: MHs; and Red: sand grains).

3 MH Under Excess-Water Conditions

3.1 MH Formation Procedure

Following the MH formation under excess-gas conditions aforementioned, two different procedures were used: a water saturation by replacing the excess gas in the sample by water at 7 MPa (Procedure A) or a water saturation accompanied by a temperature cycle (Procedure B). Please see [8] for more details.

3.2 MH Morphologies and Pore Habits Under Excess-Water Conditions

Water Saturation

The subsequent water saturation phase significantly decreased V_p for triaxial tests [8]. Kneafsey et al. [17] observed a similar decrease in sonic velocities when saturating the gas-saturated MHBS with water. These results suggest that water saturation modified the MH distribution at the grain scale. MHs located at grain contacts and/or at grain surfaces would be progressively converted or/and redistributed into the pore space [7].

For triaxial tests shown in Le et al. [8] the effects of water injection in gas-saturated MHBS were investigated at different MH saturations. The results indicate that this process took longer time for higher MH saturation. For some specimens (B2, B4, A3, and A4), this transformation was not complete when the subsequent step (triaxial compression for the specimens A and heating/cooling cycle for the specimens B) was applied. This may explain the higher measured values of V_p after the water saturation than the predicted values of the load-bearing model. Besides, for the two tests following the procedure A at high MH saturation (A3 and A4), even after waiting long time for the water saturation to make sure that MHBS was well saturated with water, V_p was still higher than the value predicted for the load-bearing model.

The results of MRI tests in the work of Le et al. [14] show heterogeneous water distribution along the sample height after the water saturation. Note that similar water saturation procedure was applied for triaxial tests and MRI tests [8, 13, 14]. However, for triaxial tests, water was injected from both top and bottom inlets while water was only injected from the bottom inlet for MRI tests as the sample cell was put into the MRI system. That explains why MH saturation was higher at the top of the sample compared to that at the bottom for MRI tests. Furthermore, the water injection time of MRI tests was longer than that of the triaxial tests. That could induce more MH dissociation during the water injection. MH distribution after the water saturation of triaxial tests would be more homogeneous as water was injected from both top and bottom inlets.

Temperature Cycle

Choi et al. [7] formed MHs in unsaturated sand following first the excess gas method, then injected saline water at conditions just outside of the MH stability zone for saline water and conducted a temperature cycle. It was concluded that slow saline water injection was a key to initiate the formation of non-cementing hydrates and the temperature cycle ensured this formation. *Vp* after warming (the MH dissociation) was quite high while the sample was not saturated. The MH dissociation was perhaps not completed before the MH reformation. This could explain why the difference of *Vp* after the saline water injection and that after the temperature cycle was small.

In the present work [8, 13, 14], normal water was injected to saturate the sample and MHs were completely dissociated before being reformed. The measurement of *Vp* at the end of the temperature cycle was smaller than that obtained after the water saturation. In addition, *Vp* at the end of the temperature cycle fitted with the pore-filling or the load-bearing model. It can then be expected that in the range of 0–50% of MH saturation, the heating/cooling cycle allows for the complete conversion of MHs with cementing pore habit into the non-cementing type either when the water saturation is not finished before the temperature cycle or when MH saturation is in a range of 40–50% (*Vp* after the complete water saturation is still higher than the value predicted for the load-bearing model).

Furthermore, MRI results [14] show more homogeneous water distribution (MH distribution) along the sample height after the temperature cycle, which suggests that the temperature cycle can redistribute MHs at the grain scale as well as at the sample scale.

To mimic natural methane hydrate-bearing marine sediments, the dissolved gas method is considered as the best method but it was time-consuming especially at high

MH saturation due to the low solubility of methane gas in water [18]. The water-excess method, proposed by Priest et al. [6], was suggested to create load-bearing MHs in sandy sediments at MH saturation lower than 40% according to sonic wave velocity measurements. However, MH was observed to be formed heterogeneously inside their sample via XRCT [16]. Kerkar et al. [9] confirmed patchy MH distribution and heterogeneous MH accumulation with XRCT at higher image spatial resolution. In the work of Lei et al. [11], the effect of saline water injection on the conversion/redistribution of MHs was confirmed by XRCT scans at high image spatial resolution. Furthermore, the obtained images showed round MH particles under excess-water conditions. Via SXRCT images [12] of the present work, MHs were initially formed following the excess-gas method. However, after multiple water migrations, MHs in both local excess-gas and excess-water media existed in the sample. MHs in local excess-gas media were in cementing forms (mineral coating and/or grain contacts, see Fig. 1) while round MH particles were found mixed with saline water in the pore space under excess-water conditions (Fig. 2). That confirmed the pore-filling/load-bearing distribution of MHs in excess-water media (round MH particles mixed in saline water in the pore space of porous media). It is supposed that MH distribution at the grain scale of MHBS after the water saturation at low MH saturation and after the temperature cycle of triaxial and MRI tests [8, 14] looks alike.

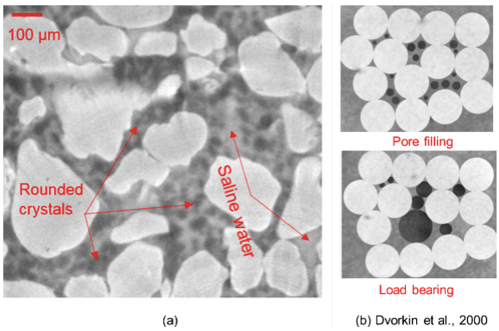

Fig. 2. (a) An example of real MH morphologies and pore habits under excess-water conditions; (b) two conceptual models proposed by Dvorkin et al. [3].

4 Mechanical Properties of MHBS

Hyodo et al. [19] shows that water-saturated sand exhibited a strain hardening and shear contraction behavior while methane hydrate-bearing sediments showed a strain softening and a shear dilation behavior. The higher the MH saturation was, the higher the strength and the more apparent the shear dilation behavior were. Furthermore, by comparing the mechanical properties of MHBS under excess-gas conditions with those under excess-water conditions (using the same sand, under the same stress conditions and at similar MH saturation) higher stiffness and higher failure strength were found for specimens under excess-gas conditions.

The experimental results obtained from triaxial tests in the present work of Le et al. [8] showed higher values for the maximum deviator stress, secant Young's modulus, residual deviator stress, and dilation angle at a higher MH saturation of MHBS under excess-water conditions [8]. Hyodo et al. [19] found similar effects of MH saturation on the maximum deviator stress and the secant Young's modulus while experimentally testing MHBS prepared following a procedure similar to the procedure A. The effects of MH saturation on the stiffness and the failure strength of MHBS were explained by particle bonding. However, the measurements of V_p in the work of Le et al. [8] suggest that cementing hydrates have been significantly converted into non-cementing types at the end of the procedure A, as explained above. In addition, the results obtained by the procedure B (where the conversion has already been completed) showed similar effects of MH saturation on the stiffness and the failure strength of MHBS. This indifference could be explained by the fact that these results were at high deformation when available MH grain bonds were broken.

5 Conclusions

In this paper, the MH formation under both excess-gas and excess-water conditions and the effects of the MH microstructure on the mechanical properties of MHBS are discussed based on the literature and the some results of the project HYDRE [13]. The following conclusions can be drawn:

MH morphologies and distribution at the grain scale of MHs under excess-gas conditions are much more complex than that described by the both cementing models (mineral coating and grain contacts) while for the media with MHs under excess-water conditions, the two idealized models (pore-filling and load-bearing) could be used to describe the MH distribution at the grain scale;

Saturating MHBS by replacing excess methane gas by water is a delicate process that can dissociate a part of MHs and redistribute MHs at the sample scale. An additional temperature cycle (under undrained conditions) makes MHs distributed more homogeneously in the sample compared to that after the water saturation. Furthermore, it is supposed that the water saturation converts (and/or redistributes) MHs in cementing form (grain contacts and/or mineral coating) to the pore space and the temperature cycle allowed for the completion of this conversion for high methane hydrate saturation samples. The MH morphologies and distribution at the grain scale of formed MHBS are supposed to be similar to that of natural MHBS (pore-filling/load-bearing habits);

The higher the MH saturation was, the higher the mechanical properties of MHBS were. However, the mechanical properties of MHBS were higher under excess-gas conditions compared to that under excess-water conditions. The effects of the temperature cycle on the physical/mechanical properties of MHBS under excess-water conditions could only be detected at high methane hydrate saturation. That is why to mimic natural methane hydrate-bearing sediments for the studies of their mechanical behaviors, with a range in MH saturation of 0–50%, the procedure A (without a temperature cycle) could be used when methane hydrate saturation was smaller than 40% to reduce the time of the MH formation, while at higher methane hydrate saturation (40–50%), a temperature cycle should be added (the procedure B should be used) to complete the MH redistribution in the pore space.

References

1. Boswell, R., Collett, T.S.: Current perspectives on gas hydrate resources. Energy Environ. Sci. **4**(4), 1206–1215 (2011)
2. Le T.X., Tang, A.M., Aimedieu, P., Bornert, M., Chabot, B., Rodts, S.: Methane hydrate-bearing sand - an energy resource? In: Randolph, M., Doan, D., Tang, A., Bui, M., Dinh, V. (eds.) Proceedings of the 1st Vietnam Symposium on Advances in Offshore Engineering. VSOE 2018. Lecture Notes in Civil Engineering, vol. 18, pp. 158–163. Springer, Singapore (2019). https://doi.org/10.1007/978-981-13-2306-5_20
3. Dvorkin, J., Helgerud, M.B., Waite, W.F., Kirby, S.H., Nur, A.: Introduction to Physical Properties and Elasticity Models. Natural Gas Hydrate. Springer, Dordrecht (2000)
4. Waite, W.F., Winters, W.J., Mason, D.H.: Methane hydrate formation in partially water-saturated Ottawa sand. Am. Miner. **89**(8–9), 1202–1207 (2004)
5. Priest, J.A., Best, A.I., Clayton, C.R.: A laboratory investigation into the seismic velocities of methane gas hydrate-bearing sand. J. Geophys. Res. Solid Earth **110**(B4) (2005)
6. Priest, J.A., Rees, E.V., Clayton, C.R.: Influence of gas hydrate morphology on the seismic velocities of sands. J. Geophys. Res. Solid Earth **114**(B11) (2009)
7. Choi, J.H., Dai, S., Cha, J.H., Seol, Y.: Laboratory formation of noncementing hydrates in sandy sediments. Geochem. Geophys. Geosyst. **15**(4), 1648–1656 (2014)
8. Le, T.X., Aimedieu, P., Bornert, M., Chabot, B., Rodts, S., Tang, A.M.: Effect of temperature cycle on mechanical properties of methane hydrate-bearing sediment. Soils Found. **59**(4), 814–827 (2019)
9. Kerkar, P.B., Horvat, K., Jones, K.W., Mahajan, D.: Imaging methane hydrates growth dynamics in porous media using synchrotron X-ray computed microtomography. Geochem. Geophys. Geosyst. **15**(12), 4759–4768 (2014)
10. Chaouachi, M., et al.: Microstructural evolution of gas hydrates in sedimentary matrices observed with synchrotron X-ray computed tomographic microscopy. Geochem. Geophys. Geosyst. **16**(6), 1711–1722 (2015)
11. Lei, L., Seol, Y., Choi, J.H., Kneafsey, T.J.: Pore habit of methane hydrate and its evolution in sediment matrix–Laboratory visualization with phase-contrast micro-CT. Mar. Pet. Geol. **104**, 451–467 (2019)
12. Le, T.X., Bornert, M., Aimedieu, P., Chabot, B., King, A., Tang, A.M.: An experimental investigation on methane hydrate morphologies and pore habits in sandy sediment using synchrotron X-ray computed tomography. Mar. Pet. Geol. **122**, 104646 (2020)
13. Le, T.X.: Experimental study on the mechanical properties and the microstructure of methane hydrate-bearing sandy sediment. PhD Thesis, Paris-Est University (2019)
14. Le, T.X., et al.: Kinetics of methane hydrate formation and dissociation in sand sediment. Geomech. Energy Environ. **23**, 100103 (2020)
15. Zhang, L., et al.: Analyzing spatially and temporally visualized formation behavior of methane hydrate in unconsolidated porous media. Magn. Reson. Imaging **61**, 224–230 (2019)
16. Zhao, J., Yang, L., Liu, Y., Song, Y.: Microstructural characteristics of natural gas hydrates hosted in various sand sediments. Phys. Chem. Chem. Phys. **17**(35), 22632–22641 (2015)
17. Kneafsey, T.J.: Examination of hydrate formation methods: trying to create representative samples (2011)
18. Spangenberg, E., Kulenkampff, J., Naumann, R., Erzinger, J.: Pore space hydrate formation in a glass bead sample from methane dissolved in water. Geophys. Res. Lett. **32**(24) (2005)
19. Hyodo, M., et al.: Mechanical behavior of gas-saturated methane hydrate-bearing sediments. J. Geophys. Res. Solid Earth **118**(10), 5185–5194 (2013)